Nitric Oxide-Generated P420 Nitric Oxide Synthase: Characterization and Roles for Tetrahydrobiopterin and Substrate in Protecting against or Reversing the P420 Conversion†

Liuxin Huang,‡ Husam M. Abu-Soud,‡ Russ Hille,§ and Dennis J. Stuehr*,‡

Department of Immunology, Lerner Research Institute, Cleveland Clinic Foundation, Cleveland, Ohio 44195, and Department of Medical Biochemistry, The Ohio State University, Columbus, Ohio 43210

Received August 13, 1998; Revised Manuscript Received December 4, 1998

ABSTRACT: The neuronal NO synthase (nNOS) heme binds self-generated NO, and this negatively regulates NO synthesis. Here we utilized the nNOS oxygenase domain and full-length nNOS along with various spectroscopic methods to (1) study formation of the six-coordinate ferrous NO complex and its conversion to a five-coordinate NO complex and (2) investigate the spectral and catalytic properties of the five-coordinate NO complex following its air oxidation to a ferric enzyme. NO bound quickly to ferrous nNOS oxygenase to form a six-coordinate NO complex (k_{on} and k_{off} values of 1.25×10^{-3} mM^{-1} s^{-1} and 128 s^{-1} at 10 °C, respectively) that was stable in the presence of L-arginine or tetrahydrobiopterin (BH_4) but was converted to a five-coordinate NO complex in a biphasic process ($k = 0.1$ and 0.01 s^{-1} at 10 °C) in the absence of these molecules. Air oxidation of the ferrous six-coordinate NO complex generated an enzyme with full activity and ferrous−CO Soret absorbance at 444 nm. In contrast, oxidation of the five-coordinate NO complex generated an inactive dimer with ferrous−CO Soret absorbance at 420 nm, indicating nNOS was converted to a ferric P420 form. Incubation of ferric P420 nNOS with BH_4 alone or BH_4 and L-arginine resulted in time-dependent reactivation of catalysis and associated recovery of P450 character. Thus, nNOS is a heme−thiolate protein that can undergo a reversible P450−P420 conversion. BH_4 has important roles in preventing P420 formation during NO synthesis, and in rescuing P420 nNOS.

Nitric oxide synthases (NOSs,[1] EC 1.14.13.39) are involved in many physiologic and pathophysiologic functions (*1*−*4*). NOSs catalyze the NADPH-dependent oxidation of L-arginine (L-Arg) to form nitric oxide (NO) and L-citrulline using O_2 as a cosubstrate. The oxidation of L-arginine proceeds in steps with N^{ω}-hydroxy-L-arginine (NHA) being formed as an intermediate (*5*, *6*). Three isoforms of NOS have been distinguished: (i) a constitutive form with a molecular mass of 160 kDa that was first isolated from rat brain (nNOS), (ii) a cytokine-inducible form with a molecular mass of 130 kDa that was first isolated from murine macrophages (iNOS), and (iii) a constitutive form with a molecular mass of 135 kDa that was first isolated from vascular endothelium (eNOS) (*7*, *8*). The enzymes are all homodimeric, with each subunit comprised of an N-terminal oxygenase domain that contains binding sites for heme, L-Arg, and tetrahydrobiopterin (BH_4) and a C-terminal reductase domain that contains binding sites for NADPH, FAD, FMN, and a central calmodulin-binding motif (*5*, *6*, *9*, *10*). Each domain can be expressed separately and can function independently of the other. For example, NOS oxygenase domains can bind L-Arg, BH_4, and O_2, and can catalyze NO synthesis from NHA in an H_2O_2-supported reaction or when provided with NADPH and their respective reductase domains (*11*−*17*).

The NOS heme is thought to play a central role in catalysis. Spectroscopic data show that the heme iron binds O_2 (*12*, *17*), presumably to catalyze its reductive activation and reaction with a terminal guanidine nitrogen of L-Arg, which is held in the distal pocket above the heme iron by a conserved glutamate residue (*18*, *19*). The NOS heme iron has a proximal thiolate ligand (*20*−*22*), as occurs in the cytochrome P450s, and the cysteine that provides the thiolate has been identified in all three NOS isoforms by mutagenesis (*11*, *23*, *24*) and crystallography (*18*). Axial thiolate ligation enables NOS to function like the cytochrome P450s in catalyzing mixed function oxidation of substrates. However, besides a common thiolate heme ligand and similar proximal heme binding loops, the heme environments in NOS and the cytochrome P450s are quite different (*18*, *19*), consistent with them being distinct heme protein monooxygenases.

The NOS heme environment may endow properties unique to NOS function and chemistry. Consider that during aerobic steady-state NO synthesis, approximately 60−90% of nNOS

† This work was supported by National Institutes of Health Grant GM51491 (D.J.S.) and a Fellowship Award from Berlex Biosciences (L.H.).

* To whom correspondence should be addressed: Immunology NN-1, Lerner Research Institute, Cleveland Clinic Foundation, 9500 Euclid Ave., Cleveland, OH 44195. Fax: (216) 444-9329. E-mail: stuehrd@cesmtp.ccf.org.

‡ Cleveland Clinic Foundation.

§ The Ohio State University.

[1] Abbreviations: BH_4, (6*R*,*S*)-5,6,7,8-tetrahydro-L-biopterin; CO, carbon monoxide; DTT, dithiothreitol; MOPS, 3-(*N*-morpholino)-propanesulfonic acid; EPR, electron paramagnetic resonance; NHA, N^{ω}-hydroxy-L-arginine; nNOS, neuronal nitric oxide synthase; nNOSoxy, oxygenase domain of nNOS; NO, nitric oxide; NOS, nitric oxide synthase.

10.1021/bi981954t CCC: $18.00
Published on Web 01/20/1999

or iNOS is present as a catalytically blocked NO complex due to them binding self-generated NO (*25*, *26*). NOS−NO complexes are stable when formed during catalysis and regenerate fully active ferric NOS upon O_2-dependent breakdown of the complex (*25*, *26*). This differentiates NOS from the cytochrome P450s which typically form unstable NO complexes that inactivate the enzyme (*27*, *28*). Reversible NO complex formation allows NO to act as a feedback inhibitor of NOS activity during the steady state, and makes the rate of NO synthesis by the enzyme proportional to the O_2 concentration throughout the physiologic range (*29*, *30*).

Evidence suggests that L-Arg and BH_4, which both bind near the heme (*19*), can stabilize the six-coordinate ferrous−NO and ferrous−CO complexes of both nNOS and iNOS. In the absence of BH_4 and L-Arg, or under BH_4-deficient conditions, NOS forms five-coordinate ferrous−NO or ferrous−CO complexes (*31*−*33*). In the case of cytochrome P450s, formation of a five-coordinate ferrous−NO complex invariably occurs after reaction with NO and leads to formation of cytochrome P420 upon air oxidation (*28*, *34*, *35*), loss of heme in some cases (*36*), and irreversible loss of activity (*27*, *28*, *34*, *36*). This inactivation process links NO synthesis with downregulation of tissue P450 activity during inflammation (*37*−*39*). However, for nNOS it is unknown if formation of a five-coordinate NO complex leads to changes in its composition, structure, or function, whether such changes could be reversed, and how BH_4 or L-Arg might influence these processes.

To address these issues, we investigated whether structural or catalytic changes would occur following air oxidation of six- and five-coordinate ferrous−NO complexes of the nNOS oxygenase domain (nNOSoxy) and full-length nNOS. This led us to characterize an inactive P420 form of nNOS, and examine whether BH_4 or L-Arg could convert this species back to an active P450 form.

MATERIALS AND METHODS

Chemicals. NHA was obtained from Alexis. NO and CO gas were purchased from Matheson Inc. BH_4 was obtained from Schircks (Jona, Switzerland). MOPS, dithionite, EDTA, L-Arg, H_2O_2, and 2-mercaptoethanol were purchased from Sigma.

Protein Expression and Purification. The nNOSoxy (amino acids 1−723 with a six-histidine tag at the C terminus) was expressed in *Escherichia coli* and purified as described previously (*12*). Full-length nNOS was expressed in *E. coli* and purified as described previously (*40*), except human calmodulin was not coexpressed, and the bacterial cultures were harvested 24 h after induction of nNOS expression. The purity of the proteins was estimated to be >85% by SDS−polyacrylamide gel electrophoresis. Both of these proteins as purified were approximately 60−80% dimeric and contain no BH_4. The heme protein concentration was estimated from the absorbance difference at 444 and 490 nm for the ferrous−CO complex using the extinction coefficient of 76 mM^{-1} cm^{-1} (*12*).

Absorption Spectral and EPR Measurements. Absorption spectral measurements were performed at 10 °C using an anaerobic cuvette. Samples containing L-Arg or BH_4 were generated by adding 10 mM L-Arg or 500 μM BH_4 to concentrated protein samples (100−300 μM) and incubating the mixtures at 4 °C overnight to allow equilibration. Diluted protein samples were made anaerobic by alternately evacuating and flushing with O_2-free argon. After the enzyme was reduced with excess dithionite, NO gas was introduced to the headspace in the anaerobic cuvette. Absorption spectra were recorded using a Hewlett-Packard 8452A single-beam diode array spectrophotometer or a Hitachi 3110 spectrophotometer. Enzyme samples (400 μL) were removed at the indicated times from the anaerobic cuvette using a long needle gastight Hamilton syringe and placed in quartz EPR tubes which had been previously flushed with O_2-free argon and finally frozen in liquid nitrogen. EPR measurements were carried out at 110 K and at the X-band microwave frequency using a Brüker ER300 EPR spectrometer equipped with a ER035M gaussmeter and a Hewlett-Packard 5352B microwave frequency counter. Experimental conditions are given in the appropriate figure legends. A total of twenty 40 s scans were accumulated for each sample to improve the signal-to-noise ratio. The EPR spectra for pure six- and five-coordinate ferrous−NO complexes of nNOSoxy were calculated from EPR samples containing a majority of one species by a method described in the legend of Figure 2.

Stopped-Flow Experiments. Rapid kinetic measurements were carried out using a Hi-tech Ltd. stopped-flow apparatus (model SF-51). Sodium dithionite-reduced nNOSoxy (2 μM) in the absence or presence of L-Arg (2 mM) and BH_4 (10 μM) was rapidly mixed with an anaerobic solution containing different concentrations of NO at 10 °C. The formation of the ferrous−NO complex was monitored at single wavelengths as indicated in the text. Signal-to-noise ratios were improved by averaging 7−10 individual traces. The time courses were fit using a nonlinear least-squares method provided by the instrument manufacturer. Estimated k_{on} and k_{off} values for NO were derived from plots of k_{obs} versus NO concentration according to the equation $k_{obs} = k_{on}[NO] + k_{off}$.

Air Oxidation of nNOS−NO Complexes and Processing of Ferric Products. Samples of nNOSoxy or nNOS full-length proteins (~20 μM) in 2 mL of 200 mM MOPS buffer (pH 7.5) containing 1 mM DTT were placed in anaerobic cuvettes, put under an argon atmosphere, and had NO gas injected into the headspace. The NO complexes were then allowed to convert to five-coordinate in the absence L-Arg and BH_4 or remain six-coordinate in the presence of these compounds. The cuvettes were then opened to air to oxidize the NO complexes. In some cases, CO was bubbled into the sample immediately after air oxidation and dithionite added so we could record the spectrum of the reduced CO complex. In other cases, aliquots (200−300 μL) of the air-oxidized solutions were incubated at room temperature from 0 to 2 h in the presence or absence of L-Arg and BH_4. At specified times, the aliquots were then placed in a centricon 30, immediately diluted to 2 mL with chilled 40 mM MOPS buffer containing 1 mM DTT at 4 °C, and reconcentrated to 0.1 mL. This dilution and concentration step was repeated three more times. The heme concentration of each washed, concentrated sample was determined spectrophotometrically from the Soret band absorbance using an extinction coefficient for ferric nNOS of 74 mM^{-1} cm^{-1}. The washed samples were then subject to spectral analysis or catalytic assay as described.

Enzyme Activity Measurement. nNOSoxy was assayed in 96-well microplates at 37 °C using NHA and H_2O_2 as

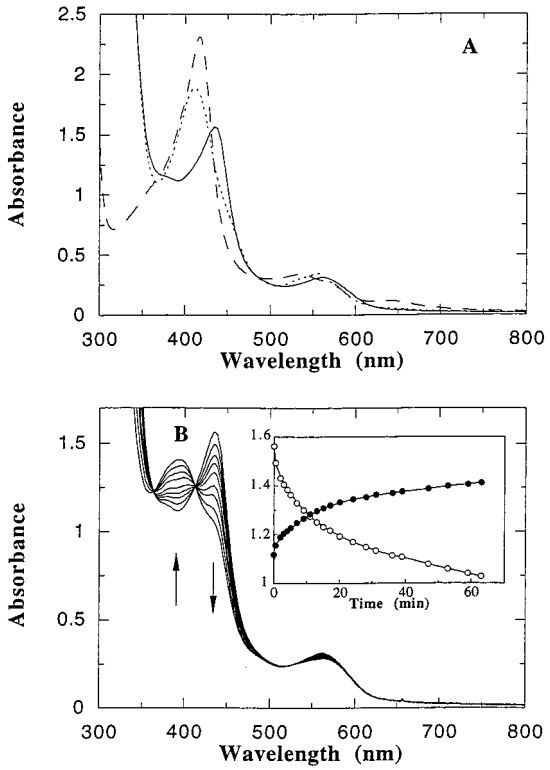

FIGURE 1: Optical absorption spectra for the ferrous nNOSoxy−NO complex. (A) The ferric (- - -), dithionite-reduced ferrous (•••), and ferrous-NO (—) forms in 0.2 M MOPS and 0.5 mM EDTA (pH 7.5). (B) Spectral change vs time for the ferrous−NO complex formed in the reaction depicted in panel A. Arrows indicate the direction of spectral change. The inset shows the time course for the change observed at 392 (●) and 436 nm (○) at 10 °C.

substrates and measuring the extent of formation of nitrite under aerobic conditions (*13*). Assays (100 μL final volume) contained 40 mM MOPS (pH 7.5), 0.5 mg/mL bovine serum albumin, 1 mM NHA, 500 μM DTT, 40 μM BH_4, 200−500 nM enzyme, and 30 mM H_2O_2. Reactions were initiated by adding H_2O_2, the mixtures incubated for 10 min at 37 °C, and the reactions stopped by adding 130 units of catalase. Assays without enzyme were used as controls. One hundred microliters of Griess reagent was then added, and the assay plate was read at 550 nm in a Thermomax plate reader. The nitrite formed was quantitated using $NaNO_2$ standards. The rate of NO synthesis by full-length nNOS was assayed using the oxyhemoglobin assay for NO as described previously (*13*).

Gel Filtration Chromatography. nNOSoxy samples were analyzed by FPLC on a 30 cm × 10 cm Pharmacia Superdex 200HR column at 4 °C. The column was equilibrated with 40 mM Tris-HCl buffer (pH 7.7) containing 1 mM DTT and 10% glycerol. Protein eluted from the column was detected at 280 nm using a flow-through detector. The apparent molecular masses of the protein peaks were estimated using gel filtration molecular mass standards as previously described (*13*).

RESULTS

Absorption Spectral and EPR Studies of Ferrous−NO Complexes. Because *E. coli* does not produce BH_4, the nNOSoxy is pterin-free. The protein has a Soret band at 416 nm (Figure 1A, dashed line), indicating that it contains a low-spin heme. When nNOSoxy was reduced with dithionite under anaerobic conditions, the ferrous form of the enzyme has absorbance maxima at 412 and 558 nm (Figure 1A, dotted line). The addition of NO gas to the ferrous enzyme results in the formation of the six-coordinate ferrous−NO complex which exhibits absorption maxima at 436 and 564 nm (Figure 1A, solid line), consistent with reported spectra for the ferrous−NO complexes of full-length iNOS and nNOS obtained in the presence of BH_4 and L-Arg (*25*, *26*). Immediately after addition of NO, an aliquot was removed and frozen and its EPR spectrum was measured at 110 K. The EPR spectrum for this sample (Figure 2A) was similar to the spectrum for the six-coordinate ferrous−NO complex of full-length nNOS (*32*) and for nNOSoxy in the presence of BH_4 and L-Arg (Figure 2E), although the comparison suggests that some five-coordinate NO complex is present in the Figure 2A spectrum.

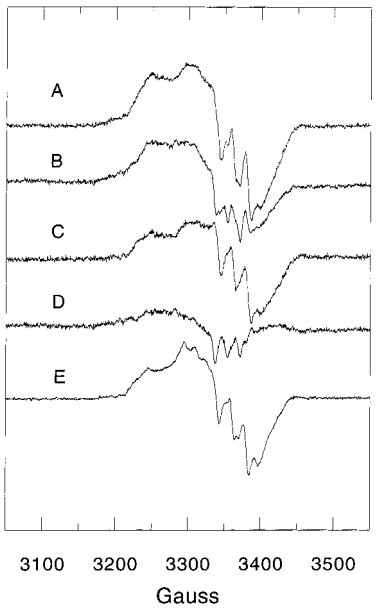

FIGURE 2: EPR spectra of ferrous−NO complexes of nNOSoxy. The enzyme concentration is about 70 μM, and the samples were maintained under anaerobic conditions. Trace A was recorded for a sample that was frozen immediately after the addition of NO gas to BH_4- and L-Arg-free, dithionite-reduced nNOSoxy at 10 °C. Trace B was recorded after the sample sat for 70 min in the presence of NO gas prior to freezing. EPR experimental conditions for traces A and B were as follows: microwave frequency, 9.457 GHz; microwave power, 10 mW; modulation amplitude, 2.012 G; and 110 K. Traces C and D are calculated spectra for the pure six- and five-coordinate ferrous−NO components, respectively, derived from traces A and B as follows. The EPR spectrum of the six-coordinate complex was obtained according to the equation six-coordinate spectrum = $A - 0.63B$. The coefficient 0.63 was set to eliminate signals in the spectrum attributed to a residual amount of five-coordinate complex. Similarly, the EPR spectrum for pure five-coordinate complex was calculated from the equation five-coordinate spectrum = $B - 0.53A$, in which the coefficient 0.53 was used to eliminate signals in the spectrum attributed to residual six-coordinate complex. Trace E is for the ferrous−NO complex of nNOSoxy formed in the presence of L-Arg and BH_4, and is included for comparison.

In the absence of L-Arg and BH_4, the absorption spectrum of the six-coordinate ferrous−NO complex changed with time. The absorbance at 436 nm decreased while that at 392 nm increased concomitantly (Figure 1B), indicating that the six-coordinate ferrous−NO complex was converting to the five-coordinate complex (*32*−*34*, *41*). After the conversion

appeared to be complete (about 70 min after addition of NO gas), another EPR spectrum was obtained (Figure 2B), which indicated that the sample contains mostly five-coordinate and some six-coordinate complex. By comparison of the EPR spectra taken immediately and 70 min after the addition of NO gas (Figure 2A,B), it is evident that the spectrum changes with time. The EPR spectra of the pure six- and five-coordinate components were calculated by difference methods explained in the Figure 2 legend, and are shown in panels C and D of Figure 2. Thus, both absorption spectral and EPR results confirm that in the absence of L-Arg and BH_4, the six-coordinate ferrous−NO complex of nNOSoxy is unstable and gradually converts to the five-coordinate complex.

To determine if L-Arg (5 mM) and BH_4 (100 μM) could convert the five-coordinate ferrous−NO complex back to the six-coordinate complex, anaerobic solutions of these molecules were added to the five-coordinate ferrous−NO complex and the mixture was incubated in a sealed cuvette at 4 °C overnight in the presence of NO. Spectral analysis indicated that <30% of the five-coordinate complex was converted to the six-coordinate ferrous−NO species under these conditions (data not shown). On the other hand, if L-Arg and BH_4 were present in a ferrous nNOSoxy sample when NO gas was first added, both absorption and EPR spectral data (Figure 2E) indicate that the six-coordinate NO complex was stable in the absence of oxygen over the same time frame, consistent with previous reports showing that L-Arg and BH_4 stabilize the six-coordinate NO complex of NOS (*25*, *32*, *33*).

Kinetics of Ferrous−NO Complex Formation and Conversion. Dithionite-reduced nNOSoxy without L-Arg and BH_4 was rapidly mixed with anaerobic solutions containing different NO concentrations at 10 °C, and the formation of the NO complex was monitored at 436 nm (*25*). Initially, the absorbance rapidly increased, consistent with formation of the six-coordinate ferrous−NO complex, and subsequently decreased more slowly, indicating conversion to the five-coordinate complex (data not shown). The data for the formation of the six-coordinate complex were best fit to a single-exponential equation, and the observed rate constants were plotted versus NO concentration (Figure 3A). The plot is linear and gives k_{on} and k_{off} values for NO binding of 1.25 $\times$ 10^3 mM^{-1} s^{-1} and 128 s^{-1}, respectively. These values are similar to NO binding constants for the iNOS oxygenase domain obtained under identical conditions (*33*). The conversion of the six-coordinate to the five-coordinate complex appeared to be biphasic, and the data were best fit to a two-exponential equation. Plots for the two sets of observed rate constants versus NO concentration (Figure 3B) show that the rate constants for the conversion of the six-coordinate to the five-coordinate complex (0.1 and 0.01 s^{-1}) are independent of NO concentration.

Spectral and Catalytic Properties of Air-Oxidized nNOSoxy NO Complexes. Because air oxidation of ferrous−NO cytochrome P450s often generates a cytochrome P420 form that is irreversibly inactivated (*34*, *35*), we tested whether air oxidation would convert NO complexes of nNOSoxy to an inactive P420 form, and if this process would be reversible. We therefore generated five- and six-coordinate ferrous−NO nNOSoxy samples,[2] exposed them to air, and

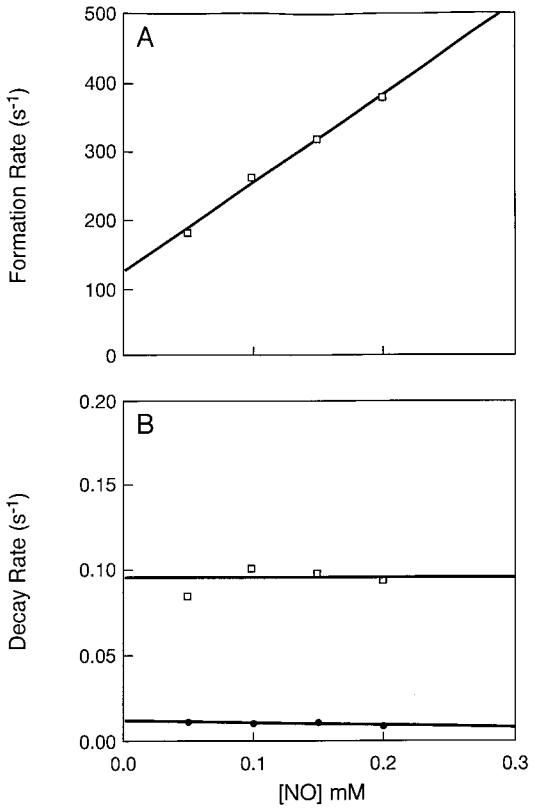

FIGURE 3: NO concentration dependence of the observed rate constants for the formation of ferrous−NO nNOSoxy in the absence of L-Arg and BH_4. Ferrous nNOSoxy (2 μM) was rapidly mixed with NO solutions at 10 °C under anaerobic conditions, and the reactions were monitored at 436 nm. (A) Plot of observed rate constants for the formation of the six-coordinate ferrous−NO complex vs the final NO concentration. (B) Plots of observed rate constants for the decay of the six-coordinate to the five-coordinate ferrous−NO complex vs the NO concentration. The two lines in panel B indicate that conversion of the six-coordinate to the five-coordinate complex is biphasic.

examined their spectral and catalytic properties after incubating the protein samples in buffer alone or in buffer containing L-Arg, BH_4, or both molecules.

The UV−visible spectrum of an air-oxidized six-coordinate NO complex was indistinguishable from the spectrum of the as-isolated ferric nNOSoxy in the presence of L-Arg and BH_4, and upon reduction in the presence of CO displayed a Soret peak at 444 nm (data not shown), consistent with nNOSoxy remaining in its P450 form throughout the experiment (*25*). In contrast, the ferric product arising from oxidation of the five-coordinate complex (Figure 4) displayed a Soret absorbance of 416 nm in the absence or presence of added L-Arg and BH_4, and the positions of its visible bands differed from those of the as-isolated ferric enzyme (Figure 4 and Table 1). Upon dithionite reduction and CO binding, this protein was observed to primarily be a P420 form of nNOSoxy (Figure 4 and Table 1), with P450 nNOSoxy present as a minor component. Thus, air oxidation of the five-coordinate NO complex appeared to generate ferric P420 nNOSoxy.

Catalytic activities of air-oxidized nNOSoxy samples incubated under the different conditions were measured as the ability to convert NHA to nitrite in an H_2O_2-supported

[2] The six-coordinate ferrous−NO nNOSoxy sample contained 2 mM L-Arg and 10 μM BH_4.

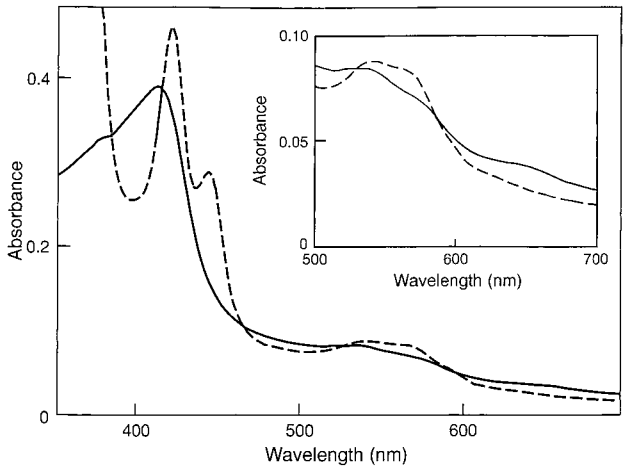

FIGURE 4: Light absorbance spectra of the air-oxidized five-coordinate NO complex of nNOSoxy (—) and its dithionite-reduced ferrous−CO complex (- - -).

Table 1: Spectral Characteristics of P450 and P420 nNOSoxy and P420CAM

protein	Soret (nm)	visible (nm)	ref
P450 nNOSoxy[a]			
ferric	417	535, 572, 650	this work
ferrous	412	558	
ferrous−CO	444, 422[c]	553	
P420 nNOSoxy[b]			
ferric	416	530, 567, 650	this work
ferrous−CO	420, 444[c]	542, 565	
P420CAM			
ferric	422	540, 566, 651	*46*
ferrous	424	530, 558	
ferrous−CO	420	540, 572	

[a] As isolated in the absence of L-Arg and BH_4. [b] Generated by air oxidation of the five-coordinate ferrous NO complex. [c] Minor component.

reaction (*13*). Control reactions showed that the amount of nitrite carried over from NO gas oxidation in the washed enzyme samples was negligible. As shown in Figure 5A, air oxidation of the six-coordinate ferrous−NO complex generated a ferric nNOSoxy that retained activity equal to that of the original enzyme sample. In contrast, an air-oxidized five-coordinate ferrous−NO sample displayed only 25% of the activity after being incubated for 2 h in buffer alone[3] (Figure 5A). However, when the air-oxidized five-coordinate sample was incubated for 2 h in buffer containing L-Arg or BH_4, it recovered 45 and 87% of the activity with respect to that of the as-isolated enzyme, and when incubated with both L-Arg and BH_4, it recovered full activity. Together, our data suggest that the ferric P420 nNOSoxy is catalytically inactive, but its activity can be recovered by incubation with L-Arg and BH_4.

Heme Environment. We next determined if loss and recovery of enzyme activity as described above were associated with changes in the nNOSoxy heme environment. A portion of each air-oxidized, incubated sample described above was reduced with sodium dithionite under a CO atmosphere to determine the relative quantities of P450 and P420 nNOSoxy. As shown in Figure 5B, the spectrum of

[3] The amount of residual activity present in four replica samples varied from 10 to 30% of that of the as-isolated enzyme and was likely due to a fraction of the ferrous−NO complex still being six-coordinate at the time of air oxidation.

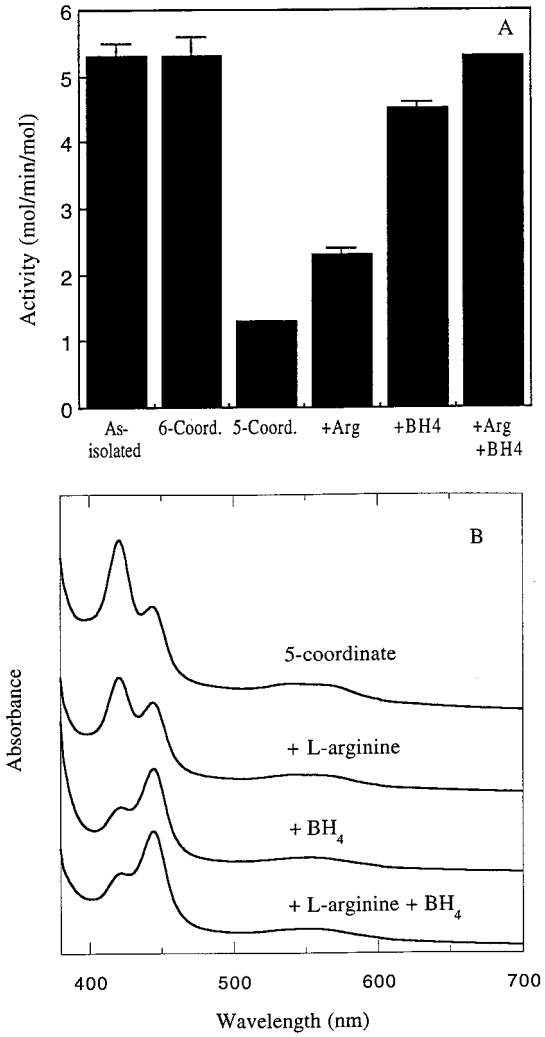

FIGURE 5: Catalytic activity of and heme iron coordination in air-oxidized NO complexes of nNOSoxy and the effect of subsequent incubation with L-Arg and BH_4. (A) Activities of the as-isolated nNOSoxy, the air-oxidized six-coordinate ferrous−NO complex, and the air-oxidized five-coordinate ferrous−NO complex after incubation with buffer alone (5-Coord.), 1 mM L-Arg (+Arg), 200 μM BH_4 (+BH4), or both L-Arg and BH_4 at room temperature for 2 h. Activity was measured as the extent of H_2O_2-dependent oxidation of NHA and is expressed as nanomoles of nitrite produced per minute per mole of heme. The data are the mean ± SD for three determinations. Panel B depicts ferrous−CO spectra for certain enzyme samples described in panel A. Spectra were recorded after incubation for 2 h under the stated conditions. Each protein sample was bubbled with CO and reduced with dithionite and the spectrum recorded immediately.

the air-oxidized enzyme that had been incubated in buffer alone contained both P420 and P450 ferrous−CO complexes, with the P420 form predominating. Samples that had been incubated in buffer containing L-Arg, BH_4, or both molecules show progressively greater proportions of the P450 ferrous−CO complex. Together, our results suggest that (1) air oxidation of the nNOSoxy five-coordinate ferrous−NO complex generates a P420 form that is catalytically inactive, (2) subsequent incubation of ferric P420 nNOSoxy with L-Arg, BH_4, or both molecules leads to recovery of the P450 form, and (3) recovery of catalytic activity is associated with recovery of P450 character.

One mechanism that could explain these results has NO binding and air oxidation causing the nNOSoxy dimer to

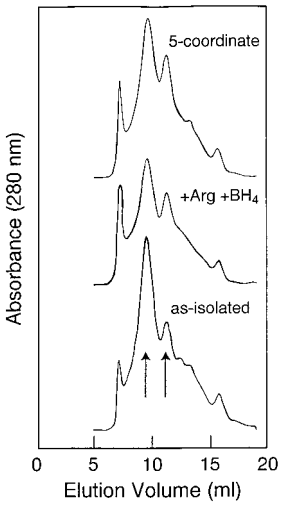

FIGURE 6: Gel filtration profiles of nNOSoxy samples. The samples were nNOSoxy as isolated, five-coordinate ferrous−NO nNOSoxy after air oxidation, and five-coordinate, air-oxidized nNOSoxy after subsequent incubation for 2 h with L-Arg and BH_4. The arrows indicate the peak positions of the nNOSoxy dimer (left) and monomer (right), on the basis of molecular mass standards. The peak eluting at ~7 mL contains protein aggregates. The data are representative of two experiments.

dissociate into heme-containing monomers, which would be expected to be catalytically inactive and form ferrous−CO complexes that quickly convert to the P420 form (*13*). To determine if nNOSoxy dimer dissociation occurred in our system, we performed gel filtration analysis on six- and five-coordinate ferrous−NO complexes following their air oxidation. The nNOSoxy samples remained primarily dimeric in all cases (Figure 6), indicating that NO-mediated catalytic inactivation of nNOSoxy and accompanying conversion to the P420 form did not arise from dissociation of the enzyme dimer.

Kinetics of Reactivation and Conversion of P420 to P450. We next examined the kinetics of catalytic reactivation and the conversion of P420 to P450 in an air-oxidized five-coordinate nNOSoxy sample during incubation at room temperature in the presence of L-Arg and BH_4. Sample aliquots were removed at various times and washed at 4 °C as described in Materials and Methods, and activity and spectral measurements were obtained. As shown in Figure 7A, recovery of nNOSoxy catalysis was gradual and required 2 h to achieve full recovery. The time course for nNOSoxy conversion from P420 to P450 was similar in the same samples (Figure 7B), and recovery of P450 character ultimately reached a level equivalent to that of the as-isolated enzyme. This confirms that BH_4- and L-Arg-induced recovery of catalytic activity is associated with recovery of P450 character.

Inactivation and Reactivation of Full-Length nNOS. So far, all the experiments were carried out using nNOSoxy. To determine if full-length nNOS was also susceptible to the NO-induced inactivation and reactivation as described above, full-length dimeric nNOS (BH_4-free) was reduced with sodium dithionite and reacted with NO under anaerobic conditions in the absence of L-Arg and BH_4. We observed a similar time-dependent conversion from the six-coordinate to the five-coordinate ferrous−NO complex (data not shown). The five-coordinate complex was then exposed to air and incubated in buffer alone or buffer containing L-Arg, BH_4,

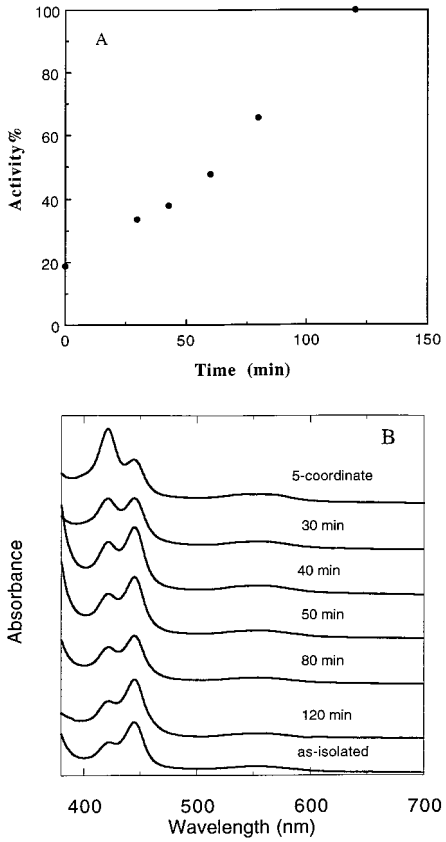

FIGURE 7: Kinetics of recovery of activity (A) and conversion of nNOSoxy P420 to P450 (B) during incubation of the air-oxidized five-coordinate NO complex with L-Arg and BH_4. The air-oxidized five-coordinate ferrous−NO complex was incubated at room temperature with 5 mM L-Arg and 200 μM BH_4; aliquots were removed at the indicated times and then washed in centricons at 4 °C prior to analysis. Panel A shows the activity of the washed samples determined as the extent of NHA conversion to nitrite in a 10 min assay. The activity of as-isolated nNOSoxy was 5 mol of nitrite per minute per mole of heme and was set at 100% for comparison. In panel B, conversion of nNOSoxy P420 to P450 during incubation with L-Arg and BH_4 was followed spectroscopically by reducing each washed enzyme sample with sodium dithionite in the presence of CO. The experiment shown is representative of three similar trials.

or both at room temperature for 2 h. Catalytic activity was measured as the rate of NADPH-supported conversion of L-Arg to NO, using the oxyhemoglobin assay. As shown in Figure 8A, the air-oxidized five-coordinate complex was completely inactive following incubation in buffer alone. Incubation with L-Arg or BH_4 resulted in recovery of 10 and 37% of the activity, respectively, while incubation with both L-Arg and BH_4 enabled full recovery of activity. A time course of catalytic recovery for full-length nNOS under the various incubation conditions (Figure 8B) indicates the recovery was gradual, as seen for nNOSoxy, and achieves either 100% recovery or intermediate recovery values depending on whether L-Arg and BH_4 were added alone or together.

Figure 9 shows results from a replica experiment with full-length nNOS in which the relative P420 and P450 character of samples incubated under the different conditions was investigated. The sample incubated in buffer alone was predominantly P420. The sample incubated with L-Arg was a mixture with the P450 form predominating, and the samples

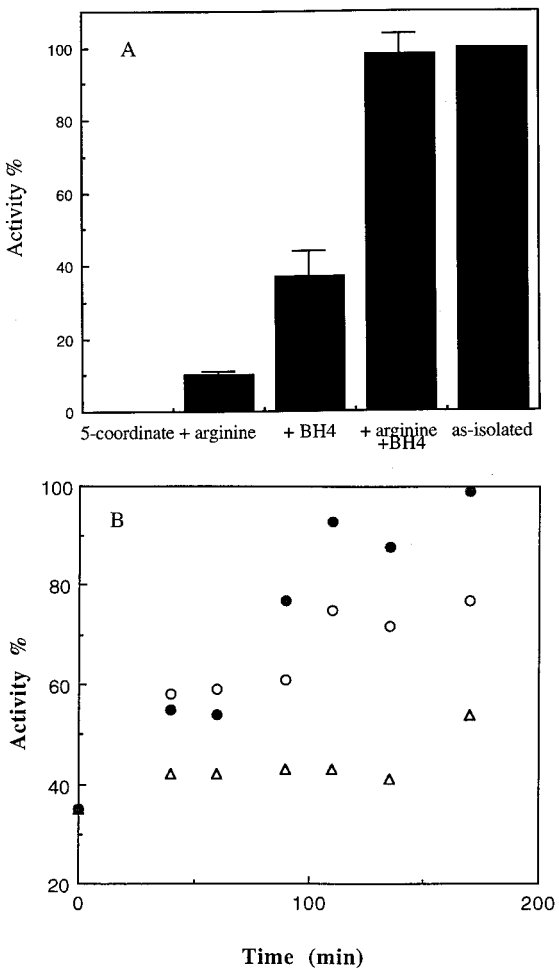

FIGURE 8: Catalytic activity and heme iron coordination in full-length nNOS after air oxidation of the five-coordinate ferrous−NO complex and the effect of subsequent incubation with L-Arg and/or BH_4. (A) Activities of the as-isolated nNOS and the air-oxidized five-coordinate ferrous−NO complex after incubation with buffer alone (5-coordinate), 1 mM L-Arg (+arginine), 200 μM BH_4 (+BH4), or both L-Arg and BH_4 at room temperature for 2 h. The activity of the as-isolated enzyme determined at room temperature using the oxyhemoglobin assay (118 nmol of NO per minute per milligram of enzyme) was set as 100%. The error bars represent the mean ± SD for three determinations. (B) Time course of catalytic recovery of the five-coordinate ferrous−NO nNOS following air oxidation and incubation with 1 mM L-Arg (△), 200 μM BH_4 (○), or both (●) at room temperature. Aliquots were removed and washed as described for nNOSoxy in Figure 7. The data are representative of two experiments.

incubated with BH_4 alone or in combination with L-Arg were almost completely in their P450 form. Thus, as was observed for nNOSoxy, NO-mediated loss of catalytic activity in full-length nNOS was associated with formation of a ferric P420 form, recovery of catalytic activity was promoted by subsequent incubation with BH_4 and L-Arg, and reactivation was associated with recovery of P450 character.

Reductase Domain Catalysis. To examine if NO inactivation of full-length nNOS also involved the nNOS reductase domain, we compared air-oxidized five-coordinate nNOS and as-isolated enzyme samples with regard to their ability to transfer electrons from NADPH to cytochrome *c*, which is a reductase domain-specific reaction (*42*). The rates of calmodulin-stimulated cytochrome *c* reduction for two air-oxidized five-coordinate nNOS samples were 90 and 97% of that of the as-isolated enzyme (data not shown). This

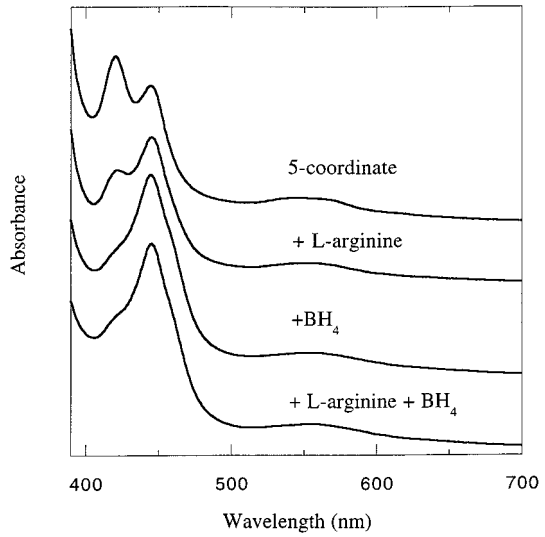

FIGURE 9: Heme iron coordination in full-length nNOS after air oxidation of the five-coordinate ferrous−NO complex and the effect of subsequent incubation with L-Arg and BH_4. Air-oxidized samples were incubated for 2 h with buffer alone (five-coordinate) or buffer containing 1 mM L-Arg, 200 μM BH_4, or both. The samples were washed in centricons, and spectra of the dithionite-reduced CO-bound forms were then recorded. The data are representative of two similar trials.

indicates that the reductase domain electron-transfer function remained intact in the NO-inhibited nNOS.

DISCUSSION

Formation and Stability of the nNOSoxy Ferrous−NO Complex. Our stopped-flow data indicate that ferrous nNOSoxy and NO combine to form a complex that is initially six-coordinate even when the reaction occurs in the absence of L-Arg and BH_4. However, under these conditions the six-coordinate complex is unstable and it converts to a species whose light absorbance and EPR spectra identify it as the five-coordinate ferrous−NO complex. Conversion from a six-coordinate to a five-coordinate ferrous−NO complex in the absence of L-Arg and BH_4 has also observed for iNOSoxy (*33*) and for full-length nNOS (*32*), and for the cytochromes P450CAM, P450LM, P450SCC, and P450NOR (*28*, *34*, *35*, *43*), suggesting nNOSoxy behaves like a typical heme−thiolate protein in this regard. However, the stability of the six-coordinate ferrous−NO complex varies widely among these proteins, taking from seconds to hours to convert to five-coordinate. In most but not all cases, the conversion is slowed by the presence of substrate. For ferrous nNOSoxy, conversion to the five-coordinate form was slowed when either L-Arg or BH_4 was present, and conversion was completely prevented in the presence of both molecules. Although L-Arg is known to stabilize the six-coordinate NO complex of full-length nNOS (*25*, *32*), a role for BH_4 had not been previously demonstrated. Our data indicate that both L-Arg and BH_4 can stabilize the ferrous heme−thiolate bond in the NO complex, although they bind at different locations relative to the heme (*19*).

Properties of the Air-Oxidized NO Complexes. Air oxidation of the ferrous nNOS five-coordinate NO complex generated a P420 form of the enzyme which although remaining dimeric did not exhibit the typical immediate spectral response toward L-Arg and BH_4 addition (Soret

Scheme 1

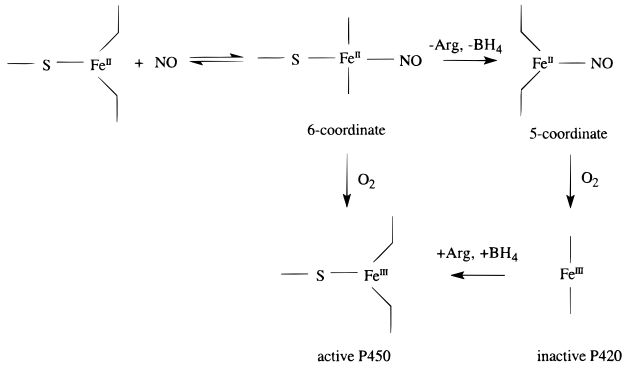

absorbance shift toward high-spin). Its light absorbance spectrum was similar but not identical to that of cytochrome P420CAM, consistent with their heme environments being somewhat distinct (*18*, *19*). P420 ferric nNOS was almost completely inactive when assayed either by H_2O_2-supported NHA oxidation (nNOSoxy) or by NADPH-supported L-Arg oxidation to NO (full-length nNOS). Inactivation required formation of the five-coordinate NO complex, because air oxidation of either the six-coordinate ferrous−NO complex or ferrous nNOSoxy control samples did not inhibit their catalysis. Inactivation was also not due to dissociation of the nNOS dimer, and appeared to only involve changes within the heme domain of nNOS, because a reductase domain-specific reaction (NADPH-dependent cytochrome *c* reduction) remained unaffected.

Reactivation of nNOS P420. NO-mediated conversion of cytochrome P450s to their P420 forms typically results in irreversible inactivation. Thus, it is remarkable that nNOS P420 could recover most or all of its activity when incubated with BH_4 alone or with BH_4 and L-Arg, respectively. Indeed, the nNOS system described here may be the clearest example to date of a heme thiolate protein undergoing P420 to P450 conversion with associated recovery of catalysis.

Catalytic recoveries of P420 nNOSoxy or P420 full-length nNOS were similar in being relatively slow and only achieving partial reactivation in the case of incubation with BH_4 or L-Arg alone. In both proteins, BH_4 promoted greater recovery of catalysis than L-Arg when added alone, and the catalytic recovery was associated with conversion from ferric P420 to P450 in all cases. However, the recovery of P450 character appeared to precede catalytic reactivation (compare panels A and B of Figure 7), and the level of P450 character achieved in certain circumstances (i.e., with L-Arg alone; see Figures 8A and 9) appeared to exceed the proportion of activity recovered in the sample. Thus, the P420 to P450 conversion may reflect an essential but singularly insufficient change in protein structure that leads to catalytic reactivation. A model consistent with the data is illustrated in Scheme 1.

It is important to note that a ferrous−CO P420 complex of NOS can form in several other settings independent of NO. For example, a P420 complex is formed when CO binds to ferrous iNOS containing BH_4 analogues tetrahydroneopterin or 6-(hydroxymethyl)tetrahydrobiopterin (*44*) or containing the NOS inhibitor 2-amino-5,6-dihydro-4*H*-1,3-thiazine (*45*). However, in these cases addition of L-Arg caused rapid conversion to the P450 CO complex. In the absence of L-Arg and BH_4, the P450 CO complex of iNOS also converts spontaneously to a P420 form (*13*, *33*). However, air oxidation of this P420 yields a ferric enzyme that is catalytically active and regenerates a P450 CO complex upon subsequent reduction. For the nNOSoxy five-coordinate ferrous−NO complex, we did not observe significant conversion to the six-coordinate NO complex even after prolonged incubation with L-Arg and BH_4 under anaerobic conditions. Furthermore, the air-oxidized product (ferric P420 nNOS) was inactive, did not respond spectrally to L-Arg and BH_4, and required prolonged incubation with these molecules to recover its P450 character and catalysis. Thus, although a P420 NOS can form by several different routes, the properties of each protein may differ depending on the conditions under which it formed.

Although we did not detect L-Arg or BH_4 binding to P420 nNOS, the fact that these molecules promote conversion to the P450 form means that they either bind to P420 nNOS without causing spectral changes or stabilize P450 nNOS if the two forms are in equilibrium. In pressure-generated cytochrome P420CAM, alterations occur in the distal pocket of the enzyme that affect ligand access to the heme and the ability of the enzyme to respond to substrate (*46*). Whether similar changes occur in NO-generated P420 nNOS will require additional study.

Relevance to NOS Biology. Understanding the properties of NOS−NO complexes is important because a major portion of iNOS and nNOS convert to their six-coordinate NO complexes during steady-state catalysis (*25*, *26*), and this conversion affects their activity versus O_2 response (*29*, *30*). Since six-coordinate NO complexes of NOS are stable in the presence of saturating BH_4 and L-Arg concentrations, cells that maintain sufficient concentrations of these molecules would be expected to avoid formation of five-coordinate NOS−NO complexes and subsequent enzyme inactivation as described in this report. However, BH_4 binding to the nNOS dimer exhibits negative cooperativity (*47*), and this allows the enzyme to be subsaturated with BH_4 over a fairly broad concentration range. Under such conditions, purified nNOS was shown to undergo NO-dependent inactivation during catalysis (*48*, *49*). Curiously, activity was restored by incubation with BH_4 but not with L-Arg (*49*). Our current work suggests that NO synthesis under BH_4-limiting conditions likely caused the nNOS−NO complex to convert to five-coordinate during the steady state, which led to accumulation of inactive ferric P420 nNOS. Whether this type of NO-based inactivation occurs in cells has not been investigated. However, it is important to consider given that the BH_4 level in some cells and tissues appears to be low enough to limit NO synthesis (*50*−*52*).

ACKNOWLEDGMENT

We thank Pam Clark for technical assistance and Craig Hemann for help with the EPR measurements.

REFERENCES

1. MacMicking, J., Xie, Q.-w., and Nathan, C. (1997) *Annu. Rev. Immunol. 15*, 323−350.
2. Harrison, D. G. (1997) *J. Clin. Invest. 100*, 2153−2157.
3. Darley-Usmar, V. M., McAndrew, J., Patel, R., Moellering, D., Lincoln, T. M., Jo, H., Cornwell, T., Digerness, S., and White, C. R. (1997) *Biochem. Soc. Trans. 25*, 919−949.
4. Loscalzo, J., and Welch, G. (1995) *Prog. Cardiovasc. Dis. 38* (2), 87−104.

5. Griffith, O. W., and Stuehr, D. J. (1995) *Annu. Rev. Physiol. 57*, 707−736.
6. Masters, B. S. S., McMillan, K., Sheta, E. A., Nishimura, J. S., Roman, L. J., and Martasek, P. (1996) *FASEB J. 10*, 552−558.
7. Knowles, R. G., and Moncada, S. (1994) *Biochem. J. 298*, 249−258.
8. Geller, D. A., and Billiar, T. R. (1998) *Cancer Metastasis Rev. 17*, 7−23.
9. Marletta, M. A. (1993) *J. Biol. Chem. 268*, 12231−12234.
10. Hemmens, B., and Mayer, B. (1997) in *Methods in Molecular Biology* (Titheradge, M. A., Ed.) Vol. 100, pp 1−32, Humana Press, Totowa, NJ.
11. McMillan, K., and Masters, B. S. S. (1995) *Biochemistry 34*, 3686−3693.
12. Abu-Soud, H. M., Gachhui, R., Raushel, F. M., and Stuehr, D. J. (1997) *J. Biol. Chem. 272*, 17349−17353.
13. Ghosh, D. K., Wu, C., Pitters, E., Molony, M., Werner, E. R., Mayer, B., and Stuehr, D. J. (1997) *Biochemistry 36*, 10609−10619.
14. Chen, P.-F., Tsai, A.-L., Berka, V., and Wu, K. K. (1996) *J. Biol. Chem. 271*, 14631−14635.
15. Gosh, D. K., Abu-Soud, H. M., and Stuehr, D. J. (1995) *Biochemistry 34*, 11316−11320.
16. Clague, M. J., Wishnok, J. S., and Marletta, M. A. (1997) *Biochemistry 36*, 14465−14473.
17. Bec, N., Gorren, A. C. F., Voelker, C., Mayer, B., and Lange, R. (1998) *J. Biol. Chem. 273*, 13502−13508.
18. Crane, B. R., Arvai, A. S., Gachhui, R., Wu, C., Ghosh, D. K., Getzoff, E. D., Stuehr, D. J., and Tainer, J. A. (1997) *Science 278*, 425−431.
19. Crane, B. R., Arvai, A. S., Ghosh, D. K., Wu, C., Getzoff, E. D., Stuehr, D. J., and Tainer, J. A. (1998) *Science 279*, 2121−2126.
20. White, K. A., and Marletta, M. A. (1992) *Biochemistry 31*, 6627−6631.
21. Wang, J., Stuehr, D. J., Ikeda-Saito, M., and Rousseau, D. L. (1993) *J. Biol. Chem. 268*, 22255−22258.
22. Sono, M., Stuehr, D. J., Ikeda-Saito, M., and Dawson, J. H. (1995) *J. Biol. Chem. 270*, 19943−19948.
23. Cubberley, R. R., Alderton, W. K., Boyhan, A., Charles, I. G., Lowe, P. N., and Old, R. W. (1997) *Biochem. J. 323*, 141−146.
24. Chen, P.-F., Tsai, A.-L., and Wu, K. K. (1994) *J. Biol. Chem. 269*, 25062−25066.
25. Abu-Soud, H. M., Wang, J., Rousseau, D. L., Fukuto, J. M., Ignarro, L. J., and Stuehr, D. J. (1995) *J. Biol. Chem. 270*, 22997−23006.
26. Hurshman, A. R., and Marletta, M. A. (1995) *Biochemistry 34*, 5627−5634.
27. Wink, D. A., Osawa, Y., Darbyshire, J. F., Jones, C. R., Eshenaur, S. C., and Nims, R. W. (1993) *Arch Biochem. Biophys. 300*, 115−123.
28. Shiro, Y., Fujii, M., Iizuka, T., Adachi, S., Tsukamoto, K., Nakahara, K., and Shoun, H. (1995) *J. Biol. Chem. 270*, 1617−1623.
29. Abu-Soud, H. M., Rousseau, D. L., and Stuehr, D. J. (1996) *J. Biol. Chem. 271*, 32515−32518.
30. Dweik, R. A., Laskowski, D., Abu-Soud, H. M., Kaneko, F. T., Hutte, R., Stuehr, D. J., and Erzurum, S. C. (1998) *J. Clin. Invest. 101*, 660−666.
31. Wang, J., Stuehr, D. J., and Rousseau, D. L. (1997) *Biochemistry 36*, 4595−4606.
32. Migita, C. T., Salerno, J. C., Masters, B. S. S., Martasek, P., McMillan, K., and Ikeda-Saito, M. (1997) *Biochemistry 36*, 10987−10992.
33. Abu-Soud, H. M., Wu, C., Ghosh, D. K., and Stuehr, D. J. (1998) *Biochemistry 37*, 3777−3786.
34. O'Keeffe, D. H., Ebel, R. E., and Peterson, J. A. (1978) *J. Biol. Chem. 253*, 3509−3516.
35. Tsubaki, M., Hiwatashi, A., Ichikawa, Y., and Hori, H. (1987) *Biochemistry 26*, 4527−4534.
36. Kim, Y.-M., Bergonia, H. A., Muller, C., Pitt, B. R., Watkins, W. D., and Lancaster, J. R., Jr. (1995) *J. Biol. Chem. 270*, 5710−5713.
37. Khatsenko, O., Gross, S. S., Rifkind, A., and Vane, J. R. (1993) *Proc. Natl. Acad. Sci. U.S.A. 90*, 11147−11151.
38. Adams, M. L., Nock, B., Truong, R., and Cicero, T. J. (1992) *Life Sci. 50*, PL-35−PL-40.
39. Stadler, J., Trockfeld, J., Schmalix, W. A., Brill, T., Siewert, J. R., Greim, H., and Doehmer, J. (1994) *Proc. Natl. Acad. Sci. U.S.A. 91*, 3559−3563.
40. Wu, C., Zhang, J., Abu-Soud, H. M., Ghosh, D. K., and Stuehr, D. J. (1996) *Biochem. Biophys. Res. Commun. 222*, 439−444.
41. Stone, J. R., Sands, R. H., Dunham, W. R., and Marletta, M. A. (1995) *Biochem. Biophys. Res. Commun. 207*, 572−577.
42. Gachhui, R., Presta, A., Bentley, D. F., Abu-Soud, H. M., McArthur, R., Brudvig, G., Ghosh, D. K., and Stuehr, D. J. (1996) *J. Biol. Chem. 271*, 20594−20602.
43. Shiro, Y., Fujii, M., Isogai, Y., Adachi, S.-i., Iizuka, T., Obayashi, E., Makino, R., Nakahara, K., and Shoun, H. (1995) *Biochemistry 34*, 9052−9058.
44. Presta, A., Siddhanta, U., Wu, C., Sennequier, N., Huang, L., Abu-Soud, H. M., Erzurum, S., and Stuehr, D. J. (1998) *Biochemistry 37*, 298−310.
45. Calaycay, J. R., Kelly, T. M., MacNaul, K. L., McCauley, E. D., Qi, H., Grant, S. K., Griffin, P. R., Klatt, T., Raju, S. M., Nussler, A. K., Shah, S., Weidner, J. R., Williams, H. R., Wolfe, G. C., Geller, D. A., Billiar, T. R., MacCoss, M., Mumford, R. A., Tocci, M. J., Schmidt, J. A., Wong, K. K., and Hutchinson, N. I. (1996) *J. Biol. Chem. 271*, 28212−28219.
46. Martinis, S. A., Blanke, S. R., Hager, L. P., Sligar, S. G., Hui Bon Hoa, G., Rux, J. J., and Dawson, J. H. (1996) *Biochemistry 35*, 14530−14536.
47. Gorren, A. C. F., List, B. M., Schrammel, A., Pitters, E., Hemmens, B., Werner, E. R., Schmidt, K., and Mayer, B. (1996) *Biochemistry 35*, 16735−16745.
48. Rengasamy, A., and Johns, R. A. (1993) *Mol. Pharmacol. 44*, 124−128.
49. Griscavage, J. M., Fukuto, J. M., Komori, Y., and Ignarro, L. J. (1994) *J. Biol. Chem. 269*, 21644−21649.
50. Cosentino, F., and Katusic, Z. S. (1995) *Circulation 91*, 139−144.
51. Tzeng, E., Billiar, T. R., Robbins, P. D., Loftus, M., and Stuehr, D. J. (1995) *Proc. Natl. Acad. Sci. U.S.A. 92*, 11771−11775.
52. Cosentino, F., Patton, S., d'Uscio, L. V., Werner, E. R., Werner-Felmayer, G., Moreau, P., Malinski, T., and Luscher, T. F. (1998) *J. Clin. Invest. 101*, 1530−1537.

BI981954T